

# INFLUENCE OF 2% TITANIUM ADDITION ON MICROSTRUCTURE AND SELECTED HIGH-TEMPERATURE PROPERTIES OF A NOVEL Co-BASED SUPERALLOY STRENGTHENED WITH L<sub>12</sub> PHASE

## WPŁYW DODATKU 2% Ti NA MIKROSTRUKTURĘ I WYBRANE WŁAŚCIWOŚCI WYSOKOTEMPERATUROWE NOWYCH NADSTOPÓW Co WZMACNIANYCH FAZĄ L<sub>12</sub>

*This paper contains selected results of primary microstructure analysis of a novel superalloy, Co-20Ni-10Al-5Mo-2Nb-2Ti. Research on this class of superalloys was started by J. Sato in 2006, and further expanded by S.K. Makineni in 2015. It is implied that Co-based, W-free superalloys will resolve the issues that the aircraft industry currently faces with Ni-based  $\gamma/\gamma'$  superalloys. It is believed that the addition of the Ti alloying element will help with  $\gamma'$  stabilisation due to high Co<sub>3</sub>(Mo, Al, Nb) fragmentation. Ti content has to be carefully selected to avoid precipitation of harmful phases, such as Co(Ti, Al).*

**Keywords:** CoNiAlMoNbTi, CoTi, casting, primary microstructure, dendrites

*Artykuł zawiera wyniki badań mikrostrukturalnych nowego nadstopu Co-20Ni-10Al-5Mo-2Nb-2Ti. Badania nad tą klasą superstopów zostały zapoczątkowane w 2006 r. przez J. Sato, a następnie rozwinięte w 2015 r. przez S.K. Makineni. Powszechna jest wiara, że nadstopy oparte na Co i wolne od W rozwiążą problemy z jakimi boryka się obecnie branża lotnicza, w której powszechne jest stosowanie nadstopów Ni  $\gamma/\gamma'$ . Uważa się, że dodatek Ti do nadstopu spowoduje stabilizację fazy  $\gamma'$  poprzez silną fragmentację fazy Co<sub>3</sub>(Mo, Al, Nb). Ilość Ti w badanym stopie została dobrana ze szczególną starannością w celu uniknięcia wydzielenia szkodliwych faz takich jak Co(Ti, Al).*

**Słowa kluczowe:** CoNiAlMoNbTi, CoTi, odlew, pierwotna mikrostruktura, dendryty

### 1. INTRODUCTION

Superalloys are a family of refractory materials characterised by exceptional physical and chemical properties. In comparison to other metallic compounds, they exhibit strong mechanical and corrosion resistance at temperatures above 1083°K. These properties make those materials promising candidates to be utilised in airplane turbo engines, turbines and nuclear reactors. [1]

Such properties are possible due to the presence of  $\gamma/\gamma'$  structure in nickel-based superalloys. This structure guarantees extraordinary creep-resistance at elevated temperatures, mainly due to blockage of dislocation movement at  $\gamma/\gamma'$  interfaces. High tensile strength, creep resistance and thermomechanical properties of the  $\gamma$ -based matrix makes it a perfect

choice for high temperature usage. Since it is based on FCC structure, the  $\gamma$  matrix has a high phase solubility, which enables the precipitation of intermetallic phases, such as  $\gamma'$ , based on L<sub>12</sub> structure [2, 3].

In order to control the precipitation process of  $\gamma'$  in superalloys, ageing was added to ensure proper creep-resistance and adequate shape of precipitates. Short ageing times lead to the formation of small, spherical particles, whereas longer ageing times cause the precipitates to have cuboid shapes, which is unique in newer superalloys. Ricks et al. determined that the exact conditions at which  $\gamma'$  shape tends to change from spherical to cuboidal are strongly dependant on lattice mismatch  $\delta$  [4].

In 2006, Sato et al. reported that a  $\gamma'$ -(L<sub>12</sub>) intermetallic phase was found in the Co-Al-W superal-

loy. This new discovery allowed the community to research a whole new subclass of cobalt-based superalloys with properties similar, if not better, than nickel-based superalloys. The growth of the newly found  $\text{Co}_3\text{Al}-(\text{L}1_2)$  phase was made possible with the addition of W [5, 6].

Despite its exceptional mechanical and corrosion resistance, the Co-Al-W superalloy is much denser ( $9.3\text{--}10.5\text{ g/cm}^3$ ) than nickel-based superalloys ( $7.9\text{--}8.5\text{ g/cm}^3$ ), and the addition of W made the alloy much harder to homogenise. These flaws led to the discovery of a W-free cobalt-based superalloy, Co-10Al-5Mo-2Nb-Ta, by S.K. Makineni et al. in 2015, which was less dense ( $8.3$  versus  $9.2\text{ g/cm}^3$ ) and exhibited a much higher yield strength than Co-Al-W ( $86$  versus  $79\text{ MPa/g}\cdot\text{cm}^3$ ). The next step in the research on W-free cobalt-based superalloys was adding nickel ( $1\text{--}30\%$ ), which enabled the increase in *solvus* temperature of up to  $124^\circ\text{K}$  ( $1139^\circ\text{K}$  to  $1263^\circ\text{K}$ ) and percentage by volume of  $\gamma'$  from  $54$  up to  $76\%$  [5, 7, 8].

The addition of Ti to Co-based, Ni doped superalloys allowed for a much stronger stabilisation of  $\gamma'$ -( $\text{L}1_2$ ). DFT calculations by Makineni et al. anticipated an increase in  $\gamma'$ -( $\text{L}1_2$ ) stability with increasing the Ti content. The experimental data confirmed the anticipations, with a *solvus* temperature increase of  $50^\circ\text{K}$  in both W-containing and W-free superalloys. This increase in *solvus* temperature was linked to a high fragmentation of  $\gamma'$  by Ti. The amount of Ti doping must be carefully selected. Higher contents of Ti present in Co-based superalloys facilitate the precipitation of harmful phases, such as  $\text{Co}_2\text{AlTi}$ , which are not coherent with the matrix and affect the mechanical properties at elevated temperatures [9–13].

Co-20Ni-10Al-5Mo-2Nb-2Ti was selected for microstructural and chemical analysis as a new, promising candidate in the Co-based W-free subclass of superalloys. This paper contains the results and discussion of LM, SEM and EBSD analysis of the Ti, Ni-doped Co-based superalloy.

## 2. MATERIAL

The sample used in the analysis was a cast  $\phi 20 \times 100\text{ mm}$  Co-20Ni-10Al-5Mo-2Nb-2Ti rod (Fig. 1). The chemical composition of the cast is shown in Table 1.

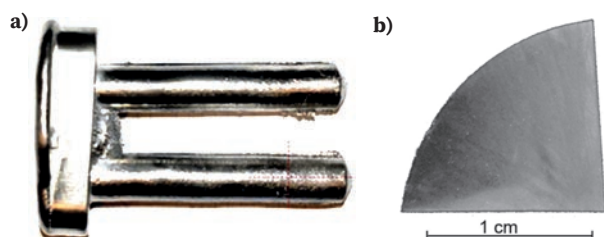


Fig. 1. Co-20Ni-10Al-5Mo-2Nb-2Ti sample: a) cast rod, b) cross-section of the cast rod

Rys. 1 Próbka Co-20Ni-10Al-5Mo-2Nb-2Ti: a) odlew, b) zgląd poprzeczny odlewu

Table 1. Chemical composition of the rod

Tabela 1. Skład chemiczny odlewu

Element	Al	Ti	Mo	Nb	Ni	Co
wt %	4.8	1.6	8.8	3.2	20.6	rest

## 3. METHODOLOGY

Optical microscope images were acquired using an Olympus DSX500i microscope. All of the observations were performed on cross-plane microsections of the cast rod. The preparation techniques included mechanical polishing and chemical etching with  $15\text{ g FeCl}_3$ ,  $150\text{ ml HCl}$  and  $300\text{ ml H}_2\text{O}$  agent. SEM images were obtained with FEI Inspect F and JEOL JSM-7200F scanning electron microscopes equipped with EDS (JEOL) detectors. TEM images were acquired with an FEI Titan 80-300 S/TEM microscope equipped with a high-resolution EDS detector and objective lens image corrector. TEM sample preparation was carried out with the use of a Struers TenuPol-5 electropolishing device and A6 electrolyte.

## 4. RESULTS

Co-20Ni-10Al-5Mo-2Nb-2Ti, as cast, has a cobalt solid solution austenitic microstructure with a small number of precipitates between interdendritic sites. Fig. 2 presents optical microscope images of colum-

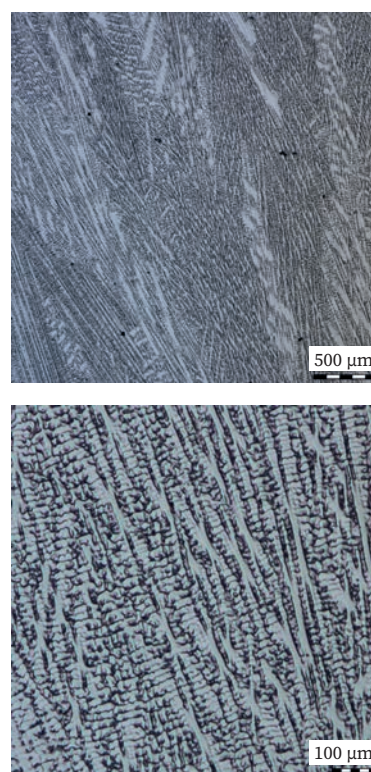
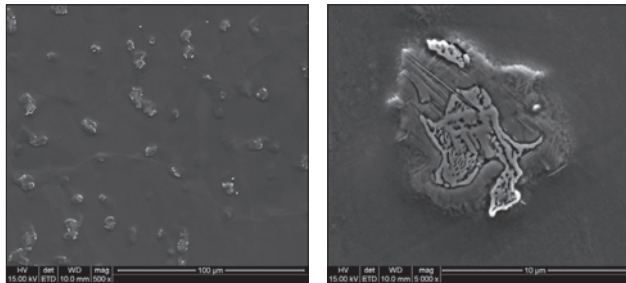


Fig. 2. Optical microscope images of Co-20Ni-10Al-5Mo-2Nb-2Ti as in cast microstructure

Rys. 2 Mikrostruktura Co-20Ni-10Al-5Mo-2Nb-2Ti w świetle mikroskopu optycznego w stanie odlewu

nal and equiaxed microstructure. The columnar crystals have elongated dendritic shapes with primary and secondary dendrites, while the equiaxed crystals are small and of random orientation. Changes in the contrast between areas of varying dendrite concentration are caused by micro segregation of alloying elements.

SEM images and EDS results are shown in Fig. 3. Precipitates in Ti-doped Co-Ni superalloys are randomly distributed and are not susceptible to grouping. Four main areas of precipitates were identified. The first area is of a typical eutectic morphology and  $\text{Co}/\text{Co}_3(\text{Al}, \text{Mo}, \text{Nb})$  formula. The second area is distributed around the first area with needle-like



Element	wt %			
	I	II	III	IV
Al	2.00	3.81	3.81	9.53
Nb	20.68	10.22	10.22	1.43
Mo	11.52	8.36	8.36	8.29
Ti	2.51	2.92	2.92	1.32
Co	51.66	55.41	55.41	63.02
Ni	11.63	19.28	19.28	20.65

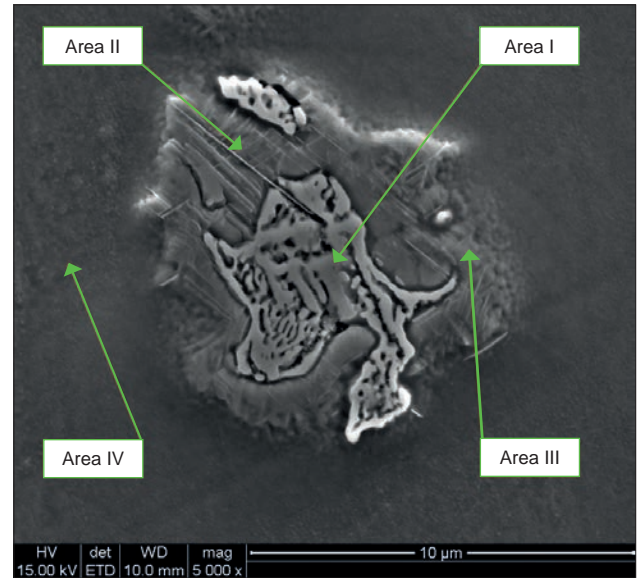


Fig. 3. SEM and EDS analysis of eutectic precipitates in Co-20Ni-10Al-5Mo-2Nb-2Ti. Four areas of varying element content are presented

Rys. 3 Analiza SEM i EDS eutektycznych wydzielen w stopie Co-20Ni-10Al-5Mo-2Nb-2Ti. Zidentyfikowano 4 obszary o różnych składach chemicznych

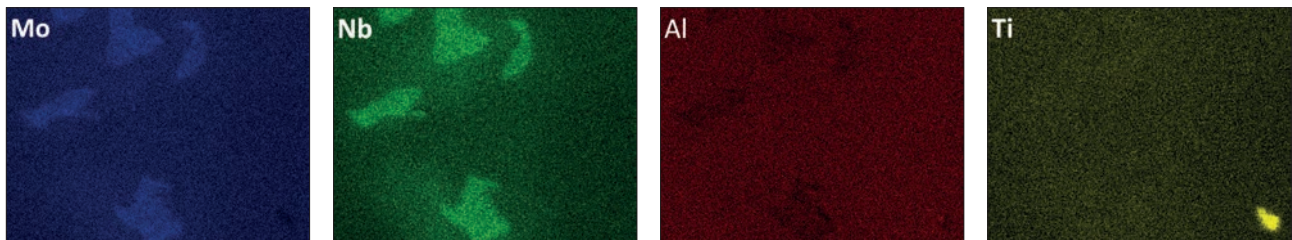


Fig. 4. EDS mapping analysis of Co-20Ni-10Al-5Mo-2Nb-2Ti

Rys. 4 Mapa EDS Co-20Ni-10Al-5Mo-2Nb-2Ti

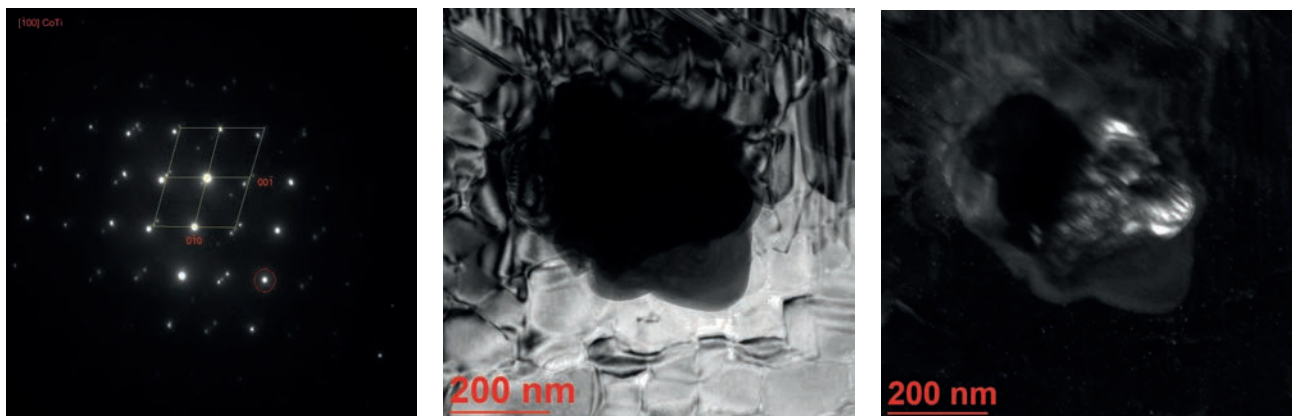


Fig. 5. TEM phase CoTi identification

Rys. 5. Identyfikacja CoTi z wykorzystaniem mikroskopu TEM

and spherical precipitates of  $\text{Co}_3\text{Mo}/\text{Co}_3\text{Nb}-(\text{D}_{019})$ . The third area does not have an eutectic shape, but is made of small, primary,  $\text{Co}_3(\text{Al}, \text{Mo}, \text{Nb})-(\text{L}_{12})$  precipitates. The fourth area contains a Co-based matrix with small  $\text{L}_{12}$  precipitates, i.e.  $\text{Co}_3(\text{Al}, \text{Mo}, \text{Nb})$ . The presence of Ti in areas I and II is not desirable for it suggests a precipitation of  $\text{Co}(\text{Al}, \text{Ti})$ , detrimental to the mechanical properties at elevated temperatures. EDS mapping of elements in the  $\text{CoAlMoNbTi}$  superalloy showed the accumulation of Mo, Nb and Al in the precipitates, further confirming the existence of  $\text{Co}_3(\text{Mo}/\text{Nb})-\text{D}_{019}$  and  $\text{Co}_3(\text{Al}, \text{Mo}, \text{Nb})-\text{L}_{12}$ . The accumulation of Al and Ti was also found to prove the existence of  $\text{CoTi}$  and  $\text{Co}_2\text{AlTi}$  in the material. The results of EDS mapping are shown in Fig. 4.

Figure 5. contains S/TEM identification of  $\text{CoTi}$ , proving its existence within the material.

## 5. CONCLUSIONS

The microstructure analysis of  $\text{Co-20Ni-10Al-5Mo-Nb-2Ti}$  proved the presence of an FCC structured Co-based matrix with interdendritic  $\gamma'-(\text{L}_{12})$  precipitates of the  $n\text{Co}_3(\text{Mo}, \text{Al}, \text{Nb})$  formula. Both columnar and equiaxed crystals have been detected.  $\gamma'$  precipitates are distributed separately and randomly.

Four main areas of precipitate morphology were identified. Undesirable Ti was found in areas I and II, where it is forming harmful  $\text{CoTi}$  precipitates identified using TEM analysis.

## REFERENCES

- [1] B. Mikulowski. *Stopy żaroodporne i żarowytrzymałe-nadstopy*. Kraków: Wydawnictwo AGH, 1997.
- [2] M.J. Donachie, S.J. Donachie. *Superalloys: A Technical Guide*. 2nd Ed. Ohio USA: ASM International, Materials Park, 2002.
- [3] T.M. Pollock, S. Tin. Nickel-Based Superalloys for Advanced Turbine Engines: Chemistry, Microstructure and Properties. *J. Propuls. Power*, 2006, 22, (2), pp. 361-374.
- [4] R.A. Ricks, A.J. Portr, R.C. Ecob. The growth of  $\gamma'$  precipitates in nickel-base superalloys. *Acta Metall.* 1983, 31(1), pp. 43-53.
- [5] J. Sato, T. Omori, K. Oikawa, I. Ohnuma, R. Kainuma, K. Ishida. Cobalt-base high-temperature alloys. *Science*, 2006, 312 (5770), pp. 90-91.
- [6] A. Suzuki, T.M. Pollock. High-temperature strength and deformation of  $\gamma/\gamma'$  two-phase Co-Al-W-base alloys. *Acta Materialia*, 2008, 56 (6), pp. 1288-1297.
- [7] S.K. Makineni, B. Nithin, K. Chattopadhyay. Synthesis of a new tungsten-free  $\gamma/\gamma'$  cobalt-based superalloy by tuning alloying additions. *Acta Mater.*, 2015, 85, pp. 85-94.
- [8] S.K. Makineni, B. Nithin, D. Palanisamy, K. Chattopadhyay. Phase evolution and crystallography of precipitates during decomposition of new tungsten-free  $\text{Co}(\text{Ni})\text{-Mo-Al-Nb } \gamma/\gamma'$  superalloys at elevated temperatures. *J. Mater. Sci.*, 2016, 51 (17), pp. 7843-7860.
- [9] M. Jiang, G. Saren, S-Y Yang, H-X Li, S-M. Hao. Phase equilibria in Co-rich region of Co-Ti-Ta system. *Trans. Nonferrous Met. Soc. China*, 2011, 21 (11), pp. 2391-2395.
- [10] D.M. Wee, O. Noguchi, Y. Oya, T. Suzuki. New  $\text{L}_{12}$  ordered alloys having the positive temperature dependence of strength. *Trans. of the Japan Institute of Metals*, 1980, 21 (4), pp. 237-247.
- [11] M. Ooshima, K. Tanaka, N.L. Okamoto, K. Kishida, H. Inui. Effects of quaternary alloying elements on the  $\gamma'$  solvus temperature of Co-Al-W based alloys with fcc/ $\text{L}_{12}$  two-phase microstructures. *J. Alloys Compd.*, 2010, 508 (1), pp. 71-78.
- [12] A. Bauer, S. Neumeier, F. Pyczak, R.F. Singer, M. Goeken. Creep properties of different  $\gamma'$  - strengthened Co-base superalloys. *Mater. Sci. Eng. A*, 2012, 550, pp. 333-341.
- [13] A. Bauer, S. Neumeier, F. Pyczak, M. Goeken. Microstructure and creep strength of different  $\gamma/\gamma'$  - strengthened Co-base superalloy variants. *Scr. Mater.*, 2010, 63 (12), pp. 1197-1200.